In vivo MEMRI brain atlas for NOD/scid-γ_c^{null} mouse model of neuroAIDS

Balasrinivasa R Sajja[1], Aditya N Bade[2], Biyun Zhou[3], Mariano G Uberti[1], Santhi Gorantla[2], Larisa Y Poluektova[2], Michael D Boska[1,2], Howard E Gendelman[2], and Yutong Liu[1,2]

[1]*Radiology, University of Nebraska Medical Center, Omaha, Nebraska, United States,* [2]*Pharmacology and Experimental Neuroscience, University of Nebraska Medical Center, Omaha, Nebraska, United States,* [3]*Anesthesiology, Tongji Medical College, Huanzhong University of Science and Technology, Wuhan, China*

INRODUCTION: Morphological phenotyping of murine models of neurodegenerative diseases provides insights into the pathobiology and treatment opportunities for human disease. The specific goal of our laboratories is to determine how the brain morphology is altered during progressive HIV-1 disease and relevant drug interventions in a humanized mouse infected with HIV-1. In order to facilitate such longitudinal studies MEMRI based *in-vivo* NOD/scid-γ_c^{null} mice (NSG) mouse brain atlas was developed. We posit through analysis of brain volumetric changes prior to HIV-1 infection we can best define the central nervous system (CNS) effects of human-mouse immune reconstitution and progressive viral infection. The NSG model is cited as amongst the most relevant reflection of human HIV-1 CNS diseases.

METHODS: **NSG mice:** Nineteen NSG mice (male, weight = 28.5 ± 2.4 grams, age = 1 year) from University of Nebraska breeding colony were used for atlas generation and as controls. **Humanization:** Five CD34-NSG mice (male, weight = 23.2 ± 1.8 grams, age = 1 year) were generated [1,2]. Human hematopoietic stem cells (HSC) for transplantation were obtained from fetal liver (University of Washington, Laboratory of Developmental Biology) or cord blood (University of Nebraska Medical Center, Department of Gynecology and Obstetrics). CD34+ HSC enriched by magnetic bead cell selection (Miltenyi Biotech Inc., Auburn, CA) were >90% pure as assessed by flow cytometry. Cells were transplanted into newborn mice irradiated at 1Gy using a C9 cobalt 60 source (Picker Corporation). HSC were injected intrahepatically at 10^5 cells/mouse. The levels of human cell engraftment were assayed in peripheral blood [2]. **MRI acquisitions:** MRI data were acquired 24 hours after $MnCl_2$ administration on Bruker Bioscan 7 Tesla/21 cm small animal scanner (Bruker, Billerica, MA) operating Paravision 4.0 with a 72 mm volume resonator and a laboratory built surface coil. Mice were anesthetized by inhalation of isoflurane in 100% oxygen and maintained 40-80 breaths/minute. Three-dimensional T1 weighted images were acquired using a spin echo sequence with the following parameters: TR/TE = 600/8 ms, number of averages = 4, image matrix = 176 × 128 × 128 with 100 µm isotropic pixel size, anterior-posterior as the readout direction. MRI data were acquired on both control and humanized mice. **Preprocessing and atlas segmentation**: All MR brain images were manually sub-imaged by separating brain from non-brain tissue. MR signal inhomogeneity was corrected [3]. An *in vivo* MEMRI based NSG brain atlas [3] was generated with 42 labeled structures and the corresponding averaged MRI were used as references for morphological effects of human immune cell transplantation. Individual mouse brain MRI was registered to the MRI atlas to compute an image deformation matrix. This deformation matrix was applied to the atlas to transfer labels onto the individual mouse MRI's allowing segmentation of brain structures. All image registration procedures were performed using Diffeomap 1.6v as implemented in DTIStudio software (www.mristudio.org).

RESULTS AND DISCUSSION: Labeled brain structures on the *in vivo* MEMRI atlas are shown (Figure A) in a cross-section of the atlas volume. A qualitative assessment of the atlas segmentation is also demonstrated (Figure B). The top row of Fig B shows a slice from average MRI and the corresponding atlas. In the second row, a slice from one of the humanized mice and overlay of transformed labels on this slice are illustrated. The segmentation procedure was applied to unaltered (n=19) and humanized (n=5) NSG mice for brain morphology. Humanized mouse brain volumes (408.93 mm^3 ± 16.56 mm^3) were significantly ($p<0.0001$) smaller compared with unmanipulated NSG mouse brain volumes (503.63 mm^3 ± 13.05 mm^3). Volumes measured as a percentage of total brain volume (Table 1, mean ± SD) showed differences between unmanipulated NSG mice and humanized NSG mice in 14 structures. It is known that the irradiation of mouse brain at birth has the effect of developmental delays on many structures [4]. However, humanization involves irradiation and human cell engrafting. Though the irradiation may be responsible for volume reduction in humanized mice, human cell engrafting may also affect the observed normalized volume changes (increase in hippocampal formation region and reduction in remaining 13 structures). This requires further investigation.

CONCLUSION: An *in vivo* MEMRI based atlas of NSG mouse brain with 42 brain sub-regions was generated to study the volumetric changes in mouse brain humanization. Understanding the pathophysiological processes involved in humanization of these mice will provide a robust background for determining effects of HIV-1 infection on brain.

Table 1: Brain structures with significantly different percentage of relative volumes in humanized and unmanipulated NSG mice.

Structure name	Unaltered (mean ± SD)	Humanized (mean ± SD)	p-value
Hypothalamus	3.777 ± 0.096	3.975 ± 0.105	0.00900
Thalamus	3.905 ± 0.089	4.148 ± 0.124	0.00866
Globus pallidus	0.626 ±0.022	0.656 ± 0.014	0.00401
Periaqueductal gray	1.508 ± 0.045	1.605 ± 0.038	0.00151
Lateral septal complex	0.877 ± 0.037	0.969 ± 0.023	0.00004
Substantia nigra	0.522 ± 0.017	0.568 ± 0.019	0.00333
Pons	3.908 ± 0.139	4.169 ± 0.115	0.00305
Anterior commissure	0.162 ± 0.005	0.171 ± 0.004	0.00526
Pallidium caudal region	0.486 ± 0.021	0.520 ± 0.011	0.00025
Pallidum medial septal nucleus	0.070 ± 0.004	0.077 ± 0.003	0.00382
Fiber tract	1.814 ± 0.047	1.882 ± 0.036	0.00764
CA1+CA2+Subiculum_HPF	3.440 ± 0.082	3.182 ± 0.121	0.00637
Epithalamus	0.173 ± 0.009	0.187 ± 0.008	0.00897
Cerebral aqueduct	0.025 ± 0.001	0.030 ± 0.002	0.00535

REFERENCES: 1. Denton PW and Garcia JV, AIDS Rev. 2011 Jul-Sep;13(3):135-48. 2. Dash PK et al. J Neurosci. 2011 Mar 2;31(9):3148-57. 3. Sajja BR et al. Proc. Intl. Soc Mag. Reson. Med. 21 (2013), #1268. 4. LM Gazdzinski et al. Int J Radiat Oncol Biol Phys. 2012 Dec 1; 84(5):e631-8.

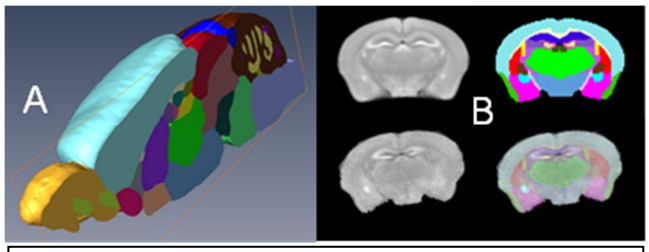

Figure A: A cross-sectional view of NSG mouse brain atlas labels. **Figure B**: Top row: A slice from averaged MRI and corresponding atlas labels. Second row: MRI slice from a humanized mouse and overlay of transformed labels on this slice after image registration.